Two photon-responsive gold nanocapsules enable targeted photothermal hyperthermia of chemoresistant melanoma: injection-route-dependent efficacy and renal evidence of fragment clearance.

Paula Zamora-Pérez[1#], Qiutian She[1#], Harrisson D. Santos[2], J. Javier Conesa[3], M. Carmen Iglesias-de la Cruz[2], Nuria Fernández[2], Daniel Jaque[2], Pilar Rivera-Gil[1,]*

[1] Integrative Biomedical Materials and Nanomedicine Lab, Department of Medicine and Life Sciences (MELIS), Pompeu Fabra University, PRBB, Carrer Doctor Aiguader 88, 08003 Barcelona, Spain.

# equally contributing authors.

* Corresponding author's e-mail: pilar.rivera@upf.edu

[2] Fluorescence Imaging Group, Departamento de Física de Materiales, Universidad Autónoma de Madrid, C/Francisco Tomás y Valiente 7, 28049 Madrid, Spain

[3] Mistral Beamline, Experiment Division, ALBA Synchrotron (ALBA-CELLS), Barcelona, Spain

SUPPORTING INFORMATION

Contents

1. Synthesis and characterization....3
2. Biological characterization....4
3. *In vivo* AuNCs-assisted photothermal therapy in murine melanoma tumors....8
4. Quantification of AuNC content after nPTT....11
5. References....11
6. Abbreviation list....12

1. Synthesis and characterization

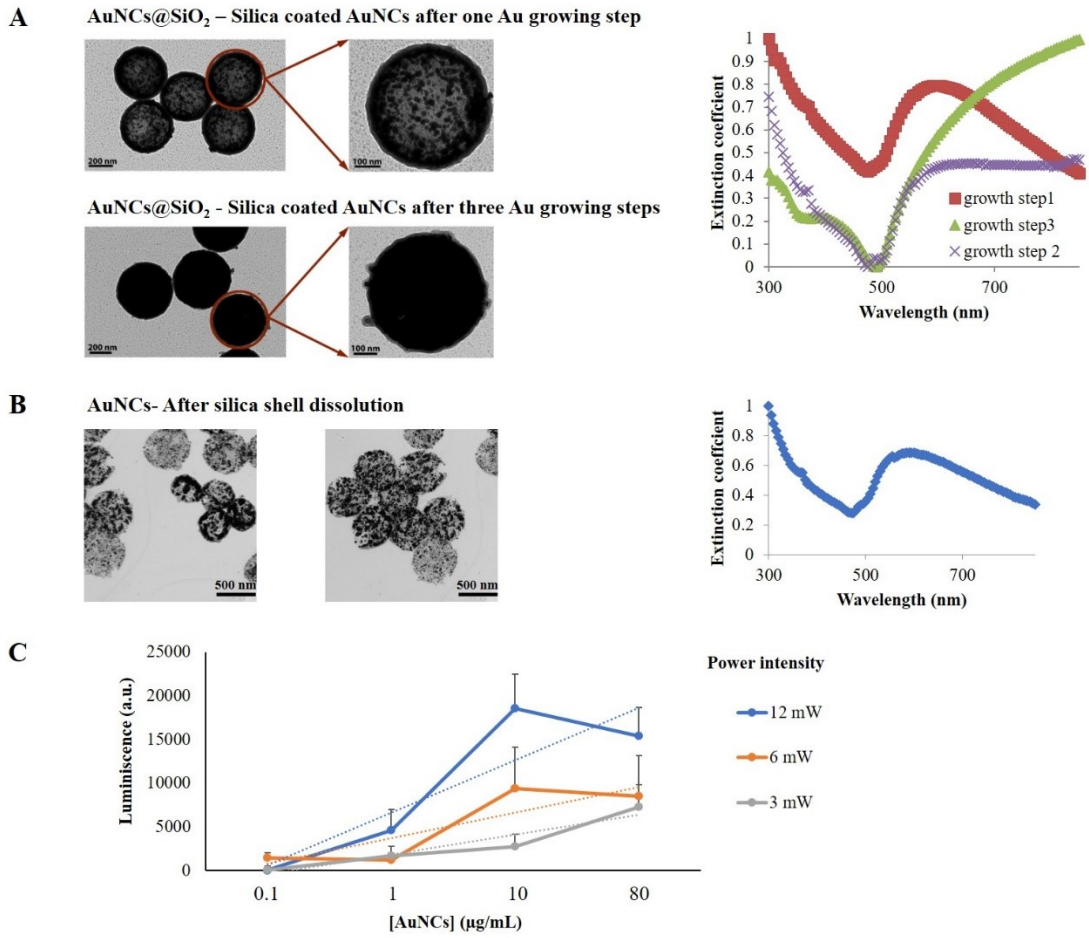

Figure SI-1. Physicochemical characterization: (A, B) Transmission electron microscopic images and the corresponding extinction (UV-vis) profile. **(C)** Multiphoton luminescence produced by different concentrations of AuNCs after multiphoton excitation (MPE) at 830 nm with 3, 6 and 12 mW power intensities which correspond to a dose range of $5.5x10^6$-$22x10^6$ Wcm^{-2}. *Abbrev: AuNCs: Gold nanocapsules.*

2. Biological characterization

Figure SI-2. *In vitro* nanoparticle-assisted photothermal therapy (nPTT) - Photothermal effect of plasmonic NCs compared to gold nanostars (AuNSs) on melanoma spheroids. (A) Dead cell counts on spheroids treated with different concentration of AuNCs and excited at different laser power intensities (see confocal images on figure 2 in the main manuscript) and on spheroids irradiated for different periods of time. The laser power intensity (3-12 mW) correspond to a focal irradiance of $5.5x10^6$-$22x10^6$ Wcm^{-2}. **(B)** TEM images of surfactant-free AuNSs (left picture). Scale bar: 100 nm. Extinction spectrum of AuNCs (blue line) and AuNSs (orange line) (right graph). **(C)** B16-F10 melanoma tumorspheres after multiphoton excitation at 830 nm (3 mW, 600 ns) without nanoparticles (control cells) and treated with AuNCs and AuNSs at equivalent doses of gold. Live cells are stained in blue, apoptotic cells are stained with phosphatidylserine (PS) in green, and necrotic cells are stained with propidium iodide in red. Scale bar: 10 µm. ***Abbrev**: AuNCs: Gold nanocapsules; AuNSs: Gold nanostars; nPTT: Nanoparticle-assisted photothermal thermal.*

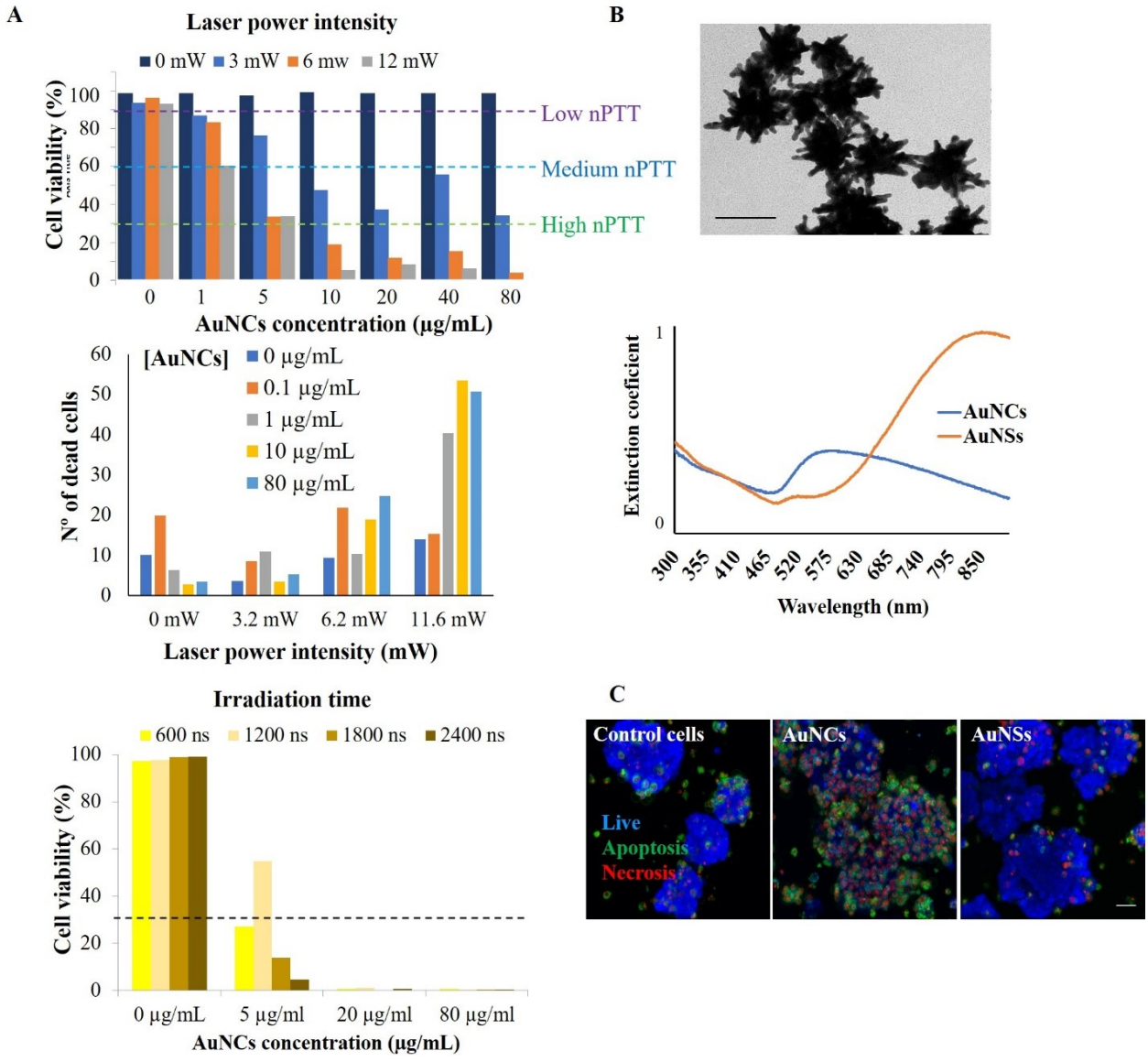

Figure SI-2 shows the response of the tumor spheroids to key parameters affecting the nPTT like AuNCs concentration, laser power and irradiation time. We studied the cell viability after 24 h by counting the number of labeled dead cells within the spheroids. It is worthy to note, the high variability of the basal level of dead cells within each tumor spheroid. This is shown in the middle graph, when comparing at 0 mW the higher number of deade cells after no AuNCs *vs* 80 µg/mL AuNCs. We observed a higher cell death with increasing AuNCs concentration and laser power. We can establish 3 nPTT areas. A low, medium, and high nPTT causing less than 10%, 40% or 70% cell death. As we excepted, no significant changes in cell viability were observed after cells were exposed to laser irradiation without AuNCs or cocultured with AuNCs without laser irradiation. AuNCs exhibited low nPTT at 1 µg/mL concentration and 3 mW laser irradiation, whereas AuNCs achieved high nPTT at 10 µg/mL AuNCs concentration and 6 mW laser irradiation.

After determination of the photothermal conditions for the successful treatment of B16-F10 melanoma spheroids, the performance of AuNCs was compared with the response of gold nanostars (AuNSs). Surfactant-free AuNSs reported photothermal agents[1] were synthesized and characterized by TEM and UV-vis spectroscopy. AuNSs presented an extinction spectrum with greater intensity than AuNCs at 830 nm where nPTT was performed. Notice the proximity to the band maximum of their LSPR at 840 nm. The TEM image showed a multi-branched AuNSs with *ca*. 110 nm of diameter. Considering that both nanomaterials had a common gold composition, their photothermal performance was evaluated at equivalent doses of gold. The quantification of gold was performed by its UV-vis absorbance at 400 nm as reported by others[2]. B16-F10 melanoma spheroids exposed to AuNCs and AuNSs at equivalent gold dose (10 µg/mL and 1.3 µM, respectively) were treated with 3 mW of two-photon excitation (2PE) (600 ns). The cellular response was assessed for live/apoptosis/necrosis markers using CytoCalcein violet 450, apopxin green and propidium iodide, respectively. CLSM images of treated spheroids evidenced that AuNCs were more effective than AuNCs to cause cellular death after nPTT at equivalent gold content. This phenomenon could be explained by the different gold distribution among NPs. While AuNCs had gold only on their external layer, AuNSs were completely solid. This conformation could imply a difference in the number of particles exposed to spheroids for interaction. Another hypothesis could be the difference in the surface of the nanomaterial relevant for cellular interaction[3]. The tips of AuNSs could interact with the plasma membrane, generating pores that do not compromise the cellular integrity after nPTT. Whereas cellular interaction with four times larger AuNCs could lead to irreversible cell damage. This could be confirmed by the cellular staining observed 10 minutes after nPTT. The nuclear staining with propidium iodide indicates cellular necrosis, probably generated by the heat of irradiated AuNCs present near the plasma membrane, which created orifices of >450 nm inducing cellular permeabilization and allowing the dye of <10 nm[4–6] to pass through the intracellular milieu. Apopxin, a small molecule with similar size, binds to phosphatidylserine (PS) generating green FL (Ex/Em: 490/525 nm) exploited for apoptosis detection. Apoptosis is characterized by the translocation of PS from the inner leaflet to the outer leaflet of the plasma membrane. Although apopxin was tested for the study of apoptotic events resultant from nPTT, considering the fast staining, it was probable that the creation of the pores allowed the fluorescent sensor to access the inner leaflet of the plasma membrane, labeling the PS.

Figure SI-3. Cellular sensitivity to paclitaxel: Paclitaxel (PTX) sensitivity of **(A)** adherent and **(B)** spheroids B16-F10 cells (*p < 0.05, ns not significant).
The cellular viability of the adherent cells and spheroids investigated using the impermeant dye, trypan blue, and CytoCalcein violet 450/propidium iodide for live/dead cell detection on adherent cells (SI-3A) and spheroids (SI-3B). The quantification of the tumor spheroids cells was calculated based on the ratio of pixels. CytoCalcein violet 450 is a dye with blue fluorescence (FL) (Ex/Em: 405/450 nm), sequestered in the cytoplasm of live cells while propidium iodide is a non-permeant dye that can only label the nucleus of the cells after loss of the integrity of plasma membrane, characteristic of cellular necrosis (Ex/Em: 546/647 nm). The total counts for each spheroid were obtained dividing the signal by the area of the spheroid. Mean ± SD is provided.

We used GraphPad prism sed for statistical analysis. The data were presented as mean value ± standard deviation (SD). The student t-test is used for unpairwise comparison. The definition of statistical significance is $p < 0.05$ applied Two-tailed calculation. (*$p < 0.05$, ns not significant).

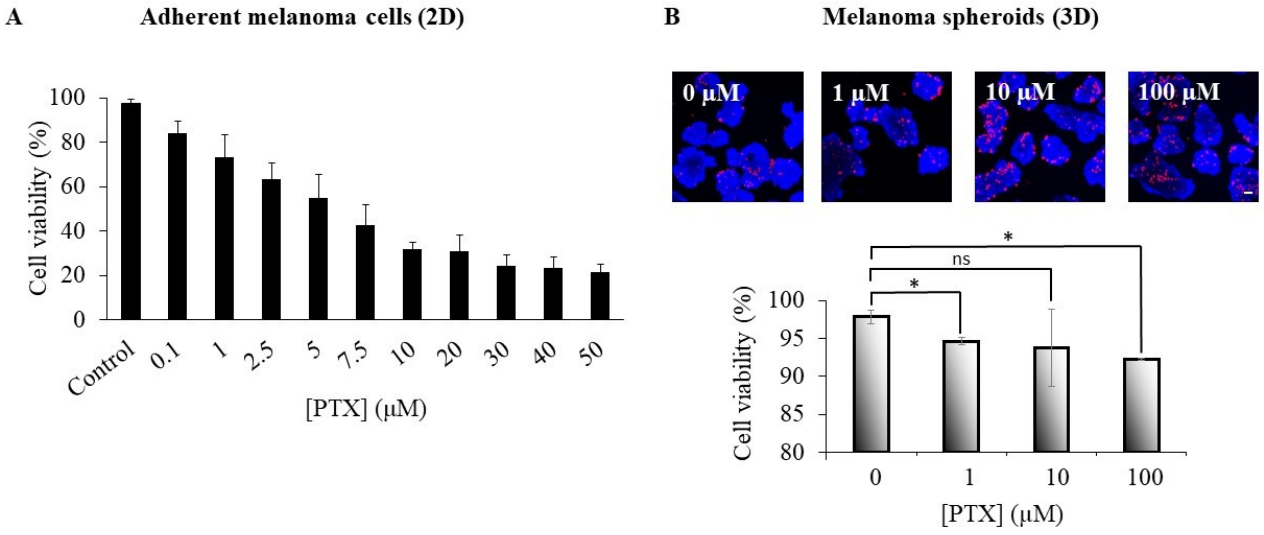

Figure SI-4. *In vitro* nanoparticle-assisted photothermal therapy enhances PTX treatment. B16-F10 cells were treated with PTX with or without concomitant AuNC-assisted photothermal therapy (AuNC, 80 μg/ml; 806-nm laser, 1 W/cm^2). Graph shows the relative cell viability. *Abbrev: PTX: Paclitaxel; nPTT: Nanoparticle-assisted photothermal therapy.*

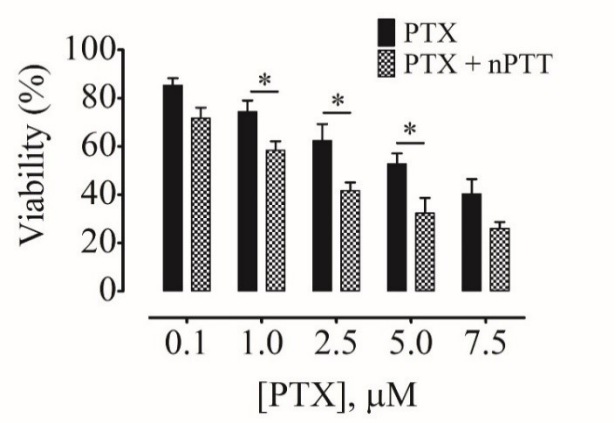

Figure SI-5. nPTT of 3D melanoma spheroids - ROS and apoptosis dynamics. Time-lapse images obtained every 5 minutes, presenting cytoplasmatic reactive oxygen species (ROS_{cyt})(pink) and apoptosis degree as indicated by PS levels (green) of B16-F10 melanoma tumorspheres **(A)** non-exposed to AuNCs and irradiated at 830 nm with MPE (3 mW) and **(B)** treated with 5 µg/mL of AuNCs and 3 mW of MPE. Zoomed images present ROS_{cyt} and PS dynamics within individual cells over time. *Abbrev.: ROS: Reactive oxygen species; PS: Phosphatidylserine; MPE: Multiphoton excitation.* Scale bar: 10 µm.

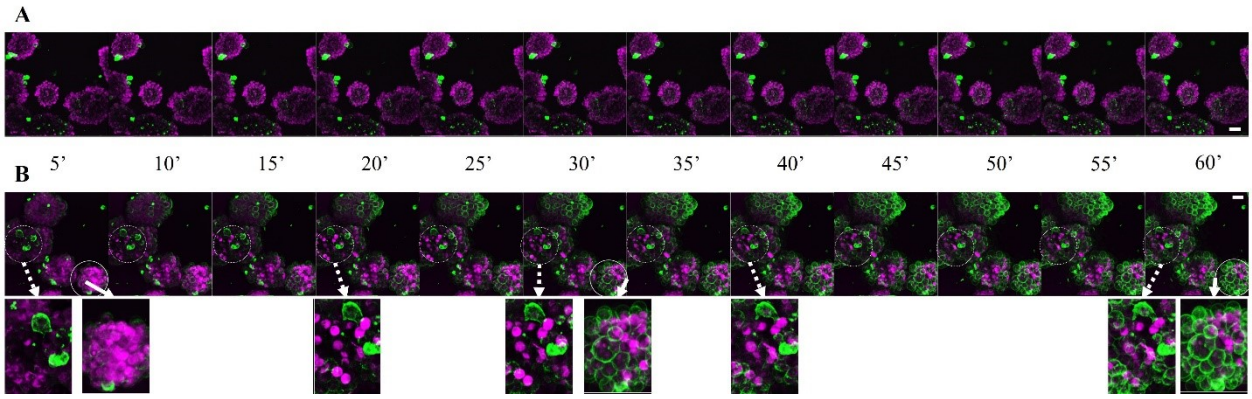

The study of ROS_{cyt} and apoptosis dynamics after 830 nm 2PE (3 mW) of B16-F10-F10 chemoresistant 3D melanoma spheroids was evaluated for 1 h and monitored by CLSM using CellROX deep red in conjunction with the PS marker, apopxin (**figure 3**). Before nPTT, ROS_{cyt} is relatively constant and there aren't evident signs of apoptosis (**figure SI-5A**). Immediately after nPTT of spheroids exposed to 5 µg/mL of AuNCs, we can detect a drop in ROS_{cyt} and increased levels of inner PS (**figure SI-5B**).

Figure SI-6. Soft X-ray tomography (cryoSXT) of cells treated with nPTT. (**A)** Melanoma cells exposed to AuNCs, presenting the nucleus (NU) *(left)* or a disintegrated nucleus *(right)* after the nPTT. **(B)** cryoSXT virtual slices of two different areas of melanoma cells treated with nPTT, showing AuNCs with high contrast (black spots), and with a smaller size than AuNCs, compatible with degradation after the heat generated because of 2PE. *Abbrev.: nPTT: Nanoparticle-assisted photothermal therapy; AuNCs: Gold nanocapsules; 2PE: Two-photon excitation.* Scale bar is 20 µm.

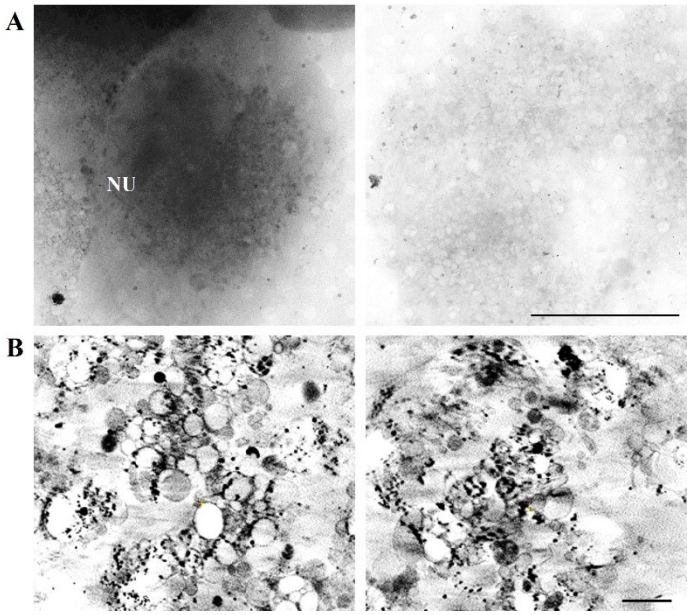

3. *In vivo* AuNCs-assisted photothermal therapy in murine melanoma tumors

Figure SI-7. General scheme of mice nPTT treatment procedure and tumor removal. Graphical description of the treatment procedure. Mice were inoculated with melanoma cells and the tumors grew for 5 days before nPTT. **(A)** Melanoma-bearing mice before and after intratumoral administration of 1 or 1.425 mg AuNCs ([AuNCs] 28.5 mg/mL; Volume 50 µL) at the injection spot highlighted in a red circle. **(B)** Mice after 24 h AuNCs administration and immediately before and after the nPTT (806 nm; 10.1 A; 1.5 cm laser spot). It is to note that the nPTT did not produce any skin burn but induces swelling and a light edema in the treated area (black dashed circle highlighted area) **(C)** Mice after 21 days post-treatment showing a scar (white dashed circle highlighted area) and complete recovery. *Abbrev.: nPTT: Nanoparticle-assisted photothermal therapy; AuNCs: Gold nanocapsules.*

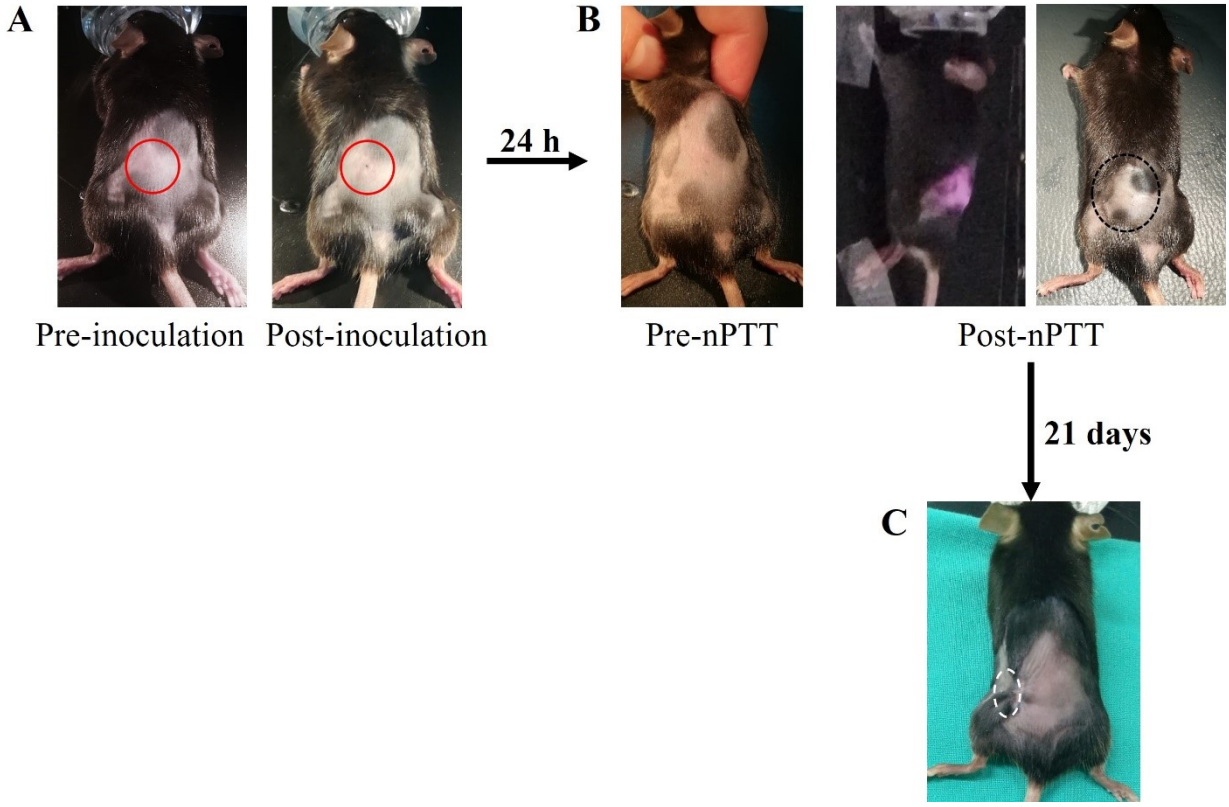

It is worthy to note that in a first attempt of nPTT, we administered the AuNCs intratumorally (IT) and we allowed them to diffuse within 1 h. This resulted in a poor distribution of the AuNCs within the tumor site, the no elimination of peritumoral cells and the reconstitution of the tumor. The tumor growth was blocked during 3 days after nPTT but regrew after that time. Therefore, we increased the diffusion time up to 24 h. Consequently, AuNCs could distribute better and the nPTT was more efficient. Resulting in tumor removal.

Figure SI-8. Real-time thermal mapping of AuNC-assisted photothermal therapy (nPTT) in B16-F10 melanoma xenografts. Female C57BL/6 mice bearing subcutaneous B16-F10 tumours (~100 mm^3) received 1 mg of AuNCs (28.5 mg mL^{-1}) either intratumorally (IT) or peritumorally (PT). One hour later the tumour area was irradiated with an 806 nm continuous-wave laser (1 W cm^{-2}, 4 min) while surface temperature was recorded with an infrared camera. **(left)** Representative thermographs of a control mouse (saline only) and an AuNC-treated mouse immediately before and at the end of irradiation; colour scale 25–57 °C. **(right)** Corresponding temperature-versus-time traces extracted from the tumour region of interest (ROI). AuNC-loaded tumours reached a plateau of ~55 °C, whereas controls stabilised at ~38 °C.

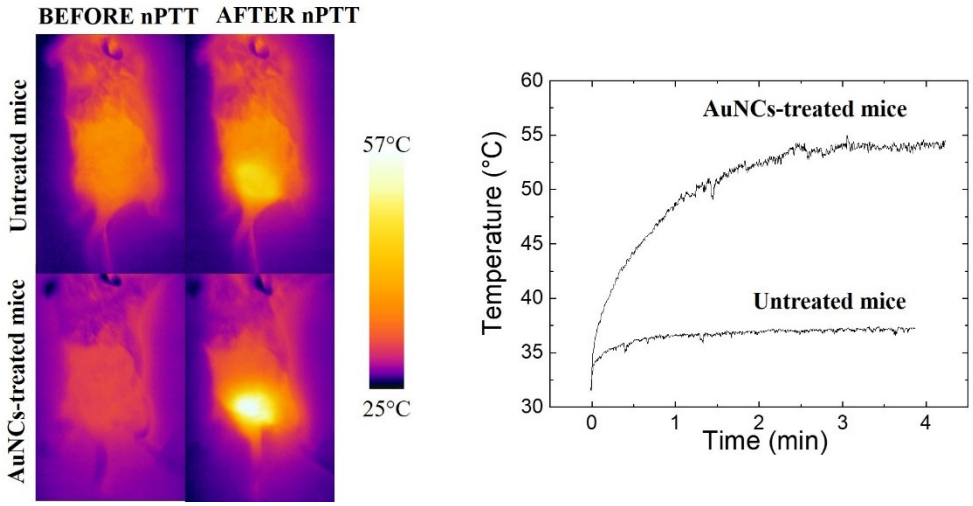

Figure SI-9. AuNCs intratumoral administration: temperature-increase live measurements at the irradiated tumor site. Mice were treated intratumorally with AuNCs and treated with nPTT. The figures show the temperature increase in the tumor immediately after nPTT and up to 4 minutes. The heat distribution within the tissue can be tracked. The maximal temperature increased from 34.7ºC (t at 0 sec.) to 64.3ºC (t at 4 min.). There is a video available as supplementary material. *Abbrev.: nPTT: Nanoparticle-assisted photothermal therapy; AuNCs: Gold nanocapsules.*

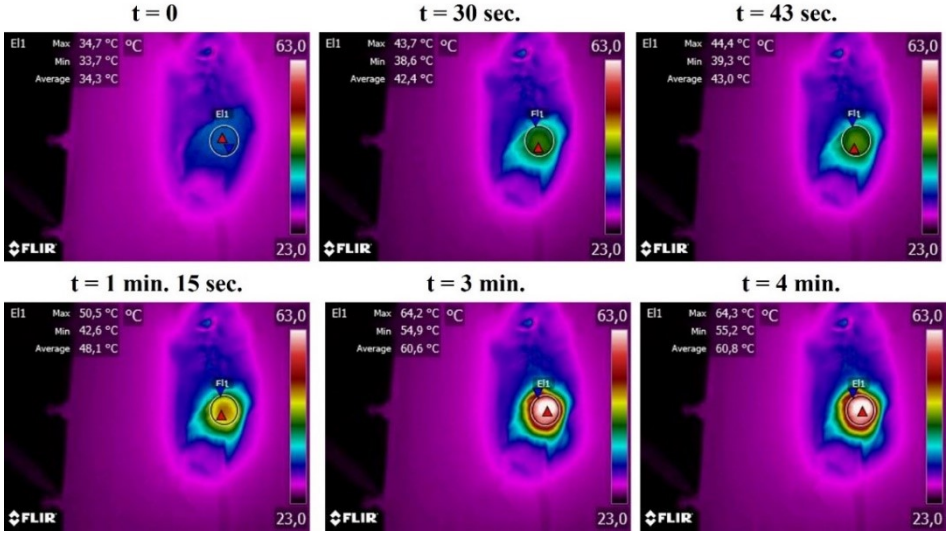

Figure SI-10. AuNCs peritumoral administration: temperature-increase live measurements at the irradiated tumor site. Mice were treated with AuNCs and treated with nPTT. The figures show the temperature increase in the tumor immediately after nPTT and up to 4 minutes. The heat distribution within the tissue can be tracked. The maximal temperature increased from 33.9ºC (t at 0 sec.) to 61.7ºC (t at 4 min.). There is a video available as supplementary material. *Abbrev.: nPTT: Nanoparticle-assisted photothermal therapy; AuNCs: Gold nanocapsules.*

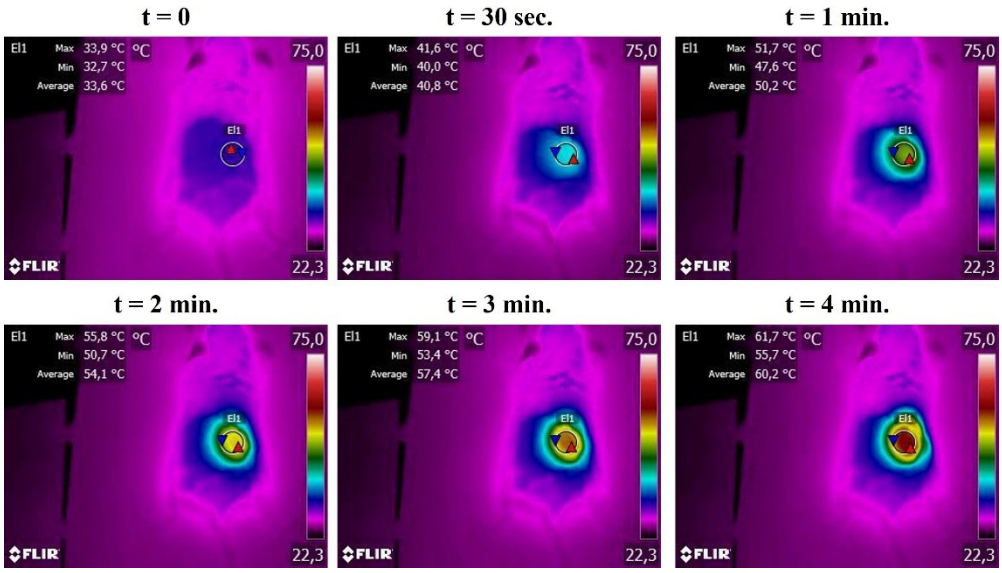

***NOTE**: Figure 4B uses a 22-75 °C colour bar, yet the FLIR overlay in SI-10 shows the hottest pixel reached 61.7 °C. The paragraph already clarifies this, but if you think the 75 °C bar might mislead readers, consider adding a parenthetical note to the figure caption itself. Aside from this cosmetic nuance, the numbers, trends and interpretations in the paragraph are fully consistent with the data presented in Figures 4, SI-8, SI-9, SI-10 and Table SI-1.*

Table SI-1. Temperature increment after IT or PT administration.

Administration route	T_max (4 min)	T_min inside heated zone (4 min)	ΔT ≈
IT (Figure 4A; SI-9)	64 °C	55 °C	27 °C
PT (Figure 4B; SI-10)	62 °C	56 °C	26 °C

Abbrev.: IT: Intratumorally; PT: Peritumoral; nPTT: Nanoparticle-assisted photothermal therapy.

4. Quantification of AuNC content after nPTT.

As can be seen in the results, the intratumoral administration of the AuNCs lead to complete tumor removal, whereas the peritumoral administration resulted in residual tumor and the formation of a scar. Interestingly, we found a signisificantly increased amount of gold from the AuNCs within all organs after the peritumoral administration being maximum in the spleen. On the contrary, after the intratumoral administration of the AuNCs the amount of gold found in the organisms was neglectable, being maximum in the scar formed after the nPTT.

A

Samples analyzed	Au content (ppm) / organ	% Injected dose	Total organ weight (g)	% Injected dose / gram of tissue
AuNCs	6621.51	100	n.a.	n.a.
Kidney	0.30	0.00458	0.2532	0.01809
Spleen	0.11	0.00169	0.0783	0.02154
Liver	0.54	0.00813	1.1324	0.00718
Blood	0.01	7.96131e-05	0.4048	0.00019
Scar	63.44	0.95808	0.2433	3.93787

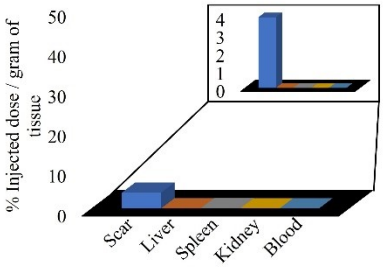

B

Samples analyzed	Au content (ppm) / organ	% Injected dose	Total organ weight (g)	% Injected dose / gram of tissue
AuNCs	6621.51	100	n.a.	n.a.
Kidney	1.40	0.02113	0.3219	0.06563
Spleen	317.91	4.80114	0.1010	47.53599
Liver	1280.00	19.33097	1.1164	17.31545
Blood	0.02	0.00030	0.6908	0.00044
Scar	n.a.	n.a.	n.a.	n.a.
Residual tumor	0.25	0.00373	0.3741	0.00996

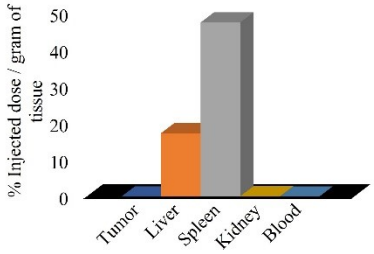

Figure SI-11. Elemental fold tissue analysis after nPTT: intratumoral *vs.* peritumoral administration. Gold content quantified *via* ICP-MS in the different nPTT-treated mice organs after **(A)** intratumoral and **(B)** peritumoral AuNCs administration. *Abbrev.: nPTT: Nanoparticle-assisted photothermal therapy; AuNCs: Gold nanocapsules; ICP-MS: Inductively coupled plasma atomic mass spectrometry.*

5. References

1 H. Yuan, C. G. Khoury, C. M. Wilson, G. A. Grant, A. J. Bennett and T. Vo-Dinh, *Nanomedicine: Nanotechnology, Biology and Medicine*, 2012, **8**, 1355–1363.2 T. Hendel, M. Wuithschick, F. Kettemann, A. Birnbaum, K. Rademann and J. Polte, *Anal. Chem.*, 2014, **86**, 11115–11124.

3 A. Verma and F. Stellacci, *Small*, 2010, **6**, 12–21.

4 H. P. Erickson, *Biol Proced Online*, 2009, **11**, 32.

5 M. M. Sadik, J. Li, J. W. Shan, D. I. Shreiber and H. Lin, *Biochimica et Biophysica Acta (BBA) - Biomembranes*, 2013, **1828**, 1322–1328.

6 S. Niekamp, J. Sung, W. Huynh, G. Bhabha, R. D. Vale and N. Stuurman, *Proceedings of the National Academy of Sciences*, 2019, **116**, 4275–4284.

6. Abbreviation list.

Abbreviation	Definition
AuNCs	Gold nanocapsules
AuNSs	Gold nanostars
CLSM	Confocal laser scanning microscopy
cryoSXT	Cryo-soft X-ray microscopy
FL	Fluorescence
ICP-MS	Inductively coupled plasma atomic mass spectrometry
LSPR	Localized surface plasmon resonance
IT	Intratumoral
nPTT	Nanoparticle-assisted photothermal therapy
NU	Nucleus
MPE	Multiphoton Excitation
2PE	Two-photon excitation
PS	Phosphatidylserine
PT	Peritumoral
PTX	Paclitaxel
ROS	Reactive Oxygen Species
ROS_{cyt}	Cytoplasmatic reactive oxygen species